Mixed-Valent Interactions in Rigid Dinuclear Systems: Electrochemical and Spectroscopic Studies of Cr^ICr^0 Ions with Controlled Torsion of the Biphenyl Bridge†

David T. Pierce‡ and William E. Geiger*

Department of Chemistry, University of Vermont, Burlington, Vermont 05405

Received August 6, 1993®

Three dinuclear complexes were prepared in which $Cr(CO)_2(PPh_3)$ moieties are connected through biphenyl linkages. The dihedral (twist) angle of the two arenes in the biphenyl decreases from 100 to 17 to 0° as the bridging ligand is changed from biphenyl-2,2′-dicarboxylic acid dimethyl ester (in compound **2**) to dihydrophenanthrene (**3**) to fluorene (**4**). All three compounds are oxidized in two reversible one-electron steps with a voltage separation of ca. 260 mV. Each monocation is shown by IR spectroscopy to be trapped-valent. ESR spectroscopy in frozen glasses gives the same result. IR sampling of the dications is achieved by low-temperature flow electrochemical experiments. The asymmetric stretching frequency of the CO pair assigned to the Cr(0) site in the mixed-valent ion is measurably shifted from that of the original Cr^0Cr^0 complex, and the amount of shift increases significantly as the biphenyl twist diminishes. It is proposed that although the half-filled orbital is localized on one metal site in the monocations, there is significant transmission of charge between the metals through filled orbitals of the biphenyl linkage. The results support a through-space model for *electronic* (mixed-valent) delocalization in $Cr^I(\mu$-biphenyl)Cr^0 linkages. Results of studies of the oxidation of (arene)$Cr(CO)_2L$, where L = CO or PPh_3, and of (biarene)$Cr_2(CO)_6$, prepared as part of this work, are briefly reported.

Introduction

This paper addresses the question of the electronic delocalization mechanism in dimetallic chromium mixed-valent ions in which the metal atoms are separated by a biphenyl spacer. The possibility that electron exchange occurs through the ligand π network is probed using model systems in which torsional twist of the biphenyl group controls the degree of π/π coupling of the two redox centers.

The factors influencing electron exchange between metal centers connected by organic ligands continue to be of considerable theoretical and practical interest.[1] Studies of this phenomenon in mixed-valent (MV) ions are often hampered by inadequate knowledge of the MV ion structures, especially as the molecular geometries might relate to the question of a through-space vs a through-bond mechanism for spin exchange. Even if the structure is known of a precursor molecule from which the mixed-valent ion is generated (e.g., by a redox process), one must allow for the possibility of important structural changes accompanying the electron-transfer process.[2] Two examples of such changes will serve to illustrate this point and lay groundwork for the studies reported in this paper.

The monocation of bis(fulvalene)diiron, BFD^+, is intrinsically delocalized.[3] The startling shortening of the Fe–Fe distance from 3.98 Å in the d^6–d^6 precursor, BFD, to 3.64 Å in the formal d^5–d^6 ion,[4] BFD^+, favors arguments for delocalization through a direct metal–metal interaction, probably by overlap of metal $d_{x^2-y^2}$ orbitals.[5] Note that, in oxidation of BFD to BFD^+, tilting of the cyclopentadienyl rings (ca. 10°) within a fulvalene unit actually decreases the amount of ligand π/π overlap in the mixed-valent complex.[4]

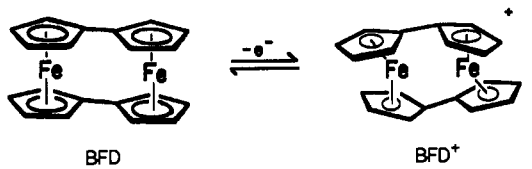

BFD BFD^+

An isoelectronic mixed-valent system also exhibiting delocalization is 1^+, the one-electron-oxidation product of (biphenyl)$Cr_2(CO)_4(\mu$-dppm), where dppm = (diphenylphosphino)methane. The metal–metal distance decreases from 4.83 Å in **1** to 4.37 Å in 1^+. Concomitant with this, however, is rotation of the biphenyls *toward* coplanarity, the dihedral angle decreasing from 50.8° in **1** to 3.7° in 1^+.[6]

The question arises as to whether the favorable overlap of the biphenyl π systems in 1^+ provides the pathway for electron delocalization. The fact that the analogue [(biphenyl)$Cr_2(CO)_4$-$(PPh_3)_2]^+$, in which the metals are presumably anti to each other, is valence trapped[6] provides no direct evidence against the involvement of the ligand π system, since the dihedral angle between the aryl groups in the ion (as well as the neutral precursor)in solution is unknown. Both biphenyl itself and

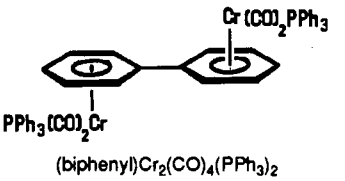

(biphenyl)$Cr_2(CO)_4(PPh_3)_2$

(biphenyl)$Cr_2(CO)_6$ have coplanar aryl groups in the solid state.[7]

† Structural Consequences of Electron-Transfer Reactions. 27. Part 26: Atwood, C.; Rheingold, A.; Geiger, W. *J. Am. Chem. Soc.* **1993**, *115*, 5310.

‡ Present address: Department of Chemistry, University of North Dakota, Grand Forks, ND 58202.

® Abstract published in *Advance ACS Abstracts,* January 1, 1994.

(1) See leading references in: (a) Marks, T. J. *Science* **1985**, *227*, 881. (b) Lee, S. *J. Am. Chem. Soc.* **1989**, *111*, 7754. (c) Jang, H. G.; Vincent, J. B.; Nakano, M.; Huffman, J. C.; Cristou, G.; Sorai, M.; Wittebort, R. J.; Hendrickson, D. N. *J. Am. Chem. Soc.* **1989**, *111*, 7778. (d) Piepho, S. B. *J. Am. Chem. Soc.* **1990**, *112*, 4197.

(2) Geiger, W. E. In *Progress in Inorganic Chemistry*; Lippard, S. J., Ed.; John Wiley and Sons: New York, 1985; Vol. 33.

(3) Levanda, C.; Bechgaard, K.; Cowan, D. O.; Mueller-Westerhoff, U. T.; Eilbracht, P.; Candela, G. A.; Collins, R. L. *J. Am. Chem. Soc.* **1976**, *98*, 3181.

(4) Hillman, M.; Kvick, A. *Organometallics* **1983**, *2*, 1780.

(5) Kirchner, R. F.; Loew, G. H.; Mueller-Westerhoff, U. T. *Inorg. Chem.* **1976**, *15*, 2665.

(6) Van Order, N., Jr.; Geiger, W. E.; Bitterwolf, T. E.; Rheingold, A. L. *J. Am. Chem. Soc.* **1987**, *109*, 5680.

(7) (a) Ohkata, K.; Paquette, R. L.; Paquette, L. A. *J. Am. Chem. Soc.* **1979**, *101*, 6687. (b) Corradini, P.; Allegra, G. *J. Am. Chem. Soc.* **1960**, *82*, 2075.

0020-1669/94/1333-0373$04.50/0

Biphenyl, however, is twisted by ca. 45° in solution.[7a] A similar twisting of the biphenyl group in (diarene)$Cr_2(CO)_4(PPh_3)_2$ would obviously diminish the π/π interactions across the spacer ligand. The possibility that electron exchange occurs through direct M–M overlap in 1^+ is also less than compelling because the M–M distance in 1^+ is much larger than that typical of a Cr–Cr bond.[8]

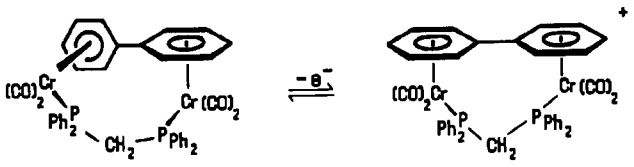

1 1^+

In the course of systematic studies designed to define the structural factors crucial to supporting electronic delocalization between metals separated by moderate distances, we first turned to the question of whether the torsion of the biphenyl group influences delocalization in these formal d^6–d^5 systems. In light of comments made in the first paragraph, we sought model systems having relatively rigid structures, so that structural characterization of the (easier to handle) precursor molecule would give information relevant also to the structure of the mixed-valent ion.

This paper reports results on three new dinuclear complexes in which the biphenyl torsion angles range from 100 to 0° in the neutral precursors, **2**–**4**. For reasons of steric origin (**2**) or of

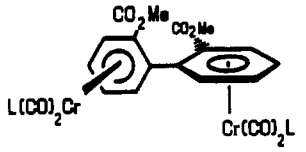

2

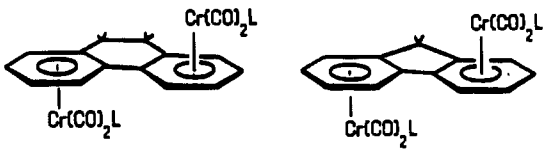

3 4

molecular rigidity (**3** and **4**), large changes in the structure of the bridging ligand are not expected to accompany the one-electron oxidation of these complexes (L = CO or PPh_3). All three complexes have an *anti* disposition of the metals, precluding direct M–M overlap. Electrochemical, IR, and ESR data establish that each of the mixed-valent ions is *valence trapped* in both frozen and ambient-temperature solutions, implying that delocalization of the half-filled orbital does *not* occur through the bridging π ligand in this set of compounds.

Experimental Section

All operations were conducted under an atmosphere of dinitrogen with thoroughly dried and freshly distilled solvents. Drybox procedures were employed for most of the electrochemical experiments; otherwise, Schlenk procedures were used. Further details are available.[9]

Electrochemistry. Most of the electrochemical procedures have been recently described.[10] Although $[Bu_4N][PF_6]$ (0.1 M) was commonly used as supporting electrolyte, some low-temperature experiments utilized $[Bu_4N][CF_3SO_3]$. The latter was prepared as described,[11] recrystallized three times from 95% EtOH, and vacuum-dried at 373 K. The laboratory reference electrodes were either the aqueous SCE or a Ag/AgCl wire, but potentials were always calibrated with an internal ferrocene or decamethylferrocene standard, and potentials in this paper are referred to the ferrocene (Fc)/ferrocenium couple, as recommended by IUPAC.[12] If desired, the reported potentials may be converted to the SCE scale by addition of +0.46 V. Only results in CH_2Cl_2 and $CH_2Cl_2/C_2H_4Cl_2$ are reported. Supplemental information concerning the behavior of the complexes in propylene carbonate and THF is available, but these solvents gave generally less satisfactory results.[9]

Spectroscopic Procedures. ^1H NMR spectra were obtained with 270- and 250-MHz Bruker Instruments; chemical shifts are reported as δ values vs TMS. ESR spectra were recorded using a modified Varian E-4 spectrometer calibrated with the diphenylpicrylhydrazyl (DPPH) radical either at 77 K for frozen solutions or at 128–250 K (±2 K) in a flow cell for fluid solutions.

IR spectra were obtained on a Nicolet series 6000 FT spectrometer operating at 2-cm^{-1} resolution. A variable-temperature flow-through IR cell with ZnS windows was employed in low-temperature experiments. The basic design of McVicar and Hubbard[13] was altered to employ a stainless steel holder and demountable transmission windows separated by a 0.5-mm Teflon spacer. A thorough description is given in the supplementary material. Temperatures down to 151 K (±1 K), monitored by a thermocouple in the solution inlet, were attained.

Solvent bands were numerically subtracted from IR absorbance spectra, and the resulting plots were normalized for analyte concentration and cell path lengths (y axis in units of $M^{-1}\,cm^{-1}$). Path lengths were measured from interference fringe patterns, which were numerically eliminated[14] from final spectra.

IR spectra of the dinuclear cations were interpreted with the aid of a computational fitting program DNMR4[15] assuming Lorentzian-shaped lines. The adaptation from NMR to IR simulations was accomplished by modeling the IR band position as δ, the integrated intensity as the nuclear population, and the line width as the inverse of T_2, as previously described.[15] We thank Dr. C. H. Bushweller for access to this program.

Monitoring of Oxidation Products. A. From Bulk Electrolyses. In order to minimize thermal decomposition of mono- and dications, electrolyses were conducted at temperatures as low as 210 K. Samples meant to be analyzed as frozen solutions by ESR were transferred to precooled tubes through a liquid-nitrogen-cooled syringe and frozen at 77 K within seconds. When 1:1 v/v $CH_2Cl_2/C_2H_4Cl_2$ was the desired medium, the CH_2Cl_2 solution was transferred into a sample tube containing an equal volume of $1,2\text{-}C_2H_4Cl_2$, and the mixture was frozen, thawed at 188 K, and refrozen at 77 K to yield transparent glassy matrices. In some cases, IR spectra of electrolysis solutions were obtained by drawing samples through cold tubing into the IR flow-cell.

B. From Chemical Oxidations. For compounds with $E°$ values negative of –0.2 V vs Fc, ferrocenium hexafluorophosphate was normally the oxidant. Complexes with more positive $E°$ values were oxidized with either $[(p\text{-}BrC_6H_4)_3N][PF_6]$, $E° = +0.84$ V vs Fc,[16] or $Ni[S_2C_2(CF_3)_2]_2$, $E° = +0.46$ V.[17] The latter has the advantage of high solubility in cold CH_2Cl_2.

Typically, 0.025 mmol of the analyte was dissolved in 1 mL of CH_2Cl_2 at 208 K. An equimolar solution of oxidant in CH_2Cl_2 prepared at ambient temperature (Fc^+, 8.6 mg in 26 mL) or 208 K $\{Ni[S_2C_2(CF_3)_2]_2$, 13.3 mg in 20 mL$\}$ was added incrementally to the analyte solution with stirring, taking care to maintain a temperature of 208 K. After ca. 1 min, the reactions were complete and the solutions were transferred either to the IR or ESR flow cells under dinitrogen pressure for liquid spectra or to precooled ESR tubes for frozen-solution spectra.

Materials. The oxidants $[Fc][PF_6]$ and $Ni[S_2C_2(CF_3)_2]_2$, $Ni(tfd)_2$, were prepared by the literature methods.[18,19] The preparation of $[(p\text{-}BrC_6H_4)_3N][PF_6]$ was a variation[20] of that reported for the $SbCl_6^-$ salt.[21]

(8) Adams, R. D.; Collins, D. E.; Cotton, F. A. *J. Am. Chem. Soc.* **1974**, *96*, 749.
(9) Pierce, D. T. Ph.D. Dissertation, University of Vermont, 1991.
(10) Pierce, D. T.; Geiger, W. E. *J. Am. Chem. Soc.* **1992**, *114*, 6063.
(11) Rouseau, K.; Farrington, G. C.; Dolphin, D. J. *J. Org. Chem.* **1972**, *37*, 3968.
(12) Gritzner, G.; Kuta, J. *Pure Appl. Chem.* **1984**, *56*, 461.
(13) McVicar, W. K. Ph.D. Dissertation, University of Vermont, 1988. We thank Dr. John L. Hubbard for aid in assembly of this apparatus.
(14) Hirchfeld, T.; Mantz, A. W. *Appl. Spectrosc.* **1976**, *30*, 552.
(15) Bushweller, C. H.; Letemdre, L. J.; Brunelle, J. A.; Bilofsky, H. S.; Whalon, M. R.; Fleischman, S. H. *Quantum Chemistry Program Exchange*; Indiana University: Bloomington, IN, 1983; Program 466.
(16) Schmidt, W.; Steckhan, E. *Chem. Ber.* **1980**, *113*, 577.
(17) Reference 19 (for CH_3CN solutions) and unpublished data by W.E.G. (CH_2Cl_2 solutions).
(18) Smart, J. C.; Pinsky, B. L. *J. Am. Chem. Soc.* **1980**, *102*, 1009.
(19) Davison, A.; Edelstein, N.; Holm, R. H.; Maki, A. H. *Inorg. Chem.* **1963**, *2*, 1227.
(20) Sheridan, P. S.; Geiger, W. E. Procedure to be published. Details will be furnished upon request.
(21) Bell, F. A.; Ledwith, A.; Sherrington, D. C. *J. Chem. Soc. C* **1969**, 2719.

All the tricarbonyl complexes, both mononuclear and dinuclear, had been previously prepared by reaction of the appropriate ligand with either $(C_6H_6)Cr(CO)_3$[22] or $Cr(CO)_6$.[23-27] The recrystallized (benzene/hexane) samples were checked for purity by elemental analysis (Robertson Laboratories, Madison, NJ), melting point, IR, NMR, and mass spectrometry (methane, CI, Finigan MAT 4500 series).

The dicarbonyl triphenylphosphine complexes were prepared by UV photolysis[28] (200-W medium-pressure Hg lamp) of water-cooled benzene or THF solutions of the proper tricarbonyl complex in the presence of PPh_3. Monometallic PPh_3 complexes were purified by chromatography on activity I silica gel, 60–200 mesh, whereas the dimetallic phosphine complexes were simply washed with acetone/hexane mixtures and recrystallized from THF/hexane. Care was taken to exclude light from reactions involving tricarbonyl complexes. Satisfactory C and H analyses were obtained for all new compounds. Typical preparations follow.

Monometallic Dicarbonyl Triphenylphosphine Complexes. (Biphenyl-2,2′-dicarboxylic acid dimethyl ester)dicarbonyl(triphenylphosphine)-chromium (5). A mixture of 0.50 g (1.23 mmol) of the tricarbonyl complex **8** and 1.0 g (3.81 mmol) of PPh_3 in 200 mL benzene was irradiated, with aliquots taken intermittently for IR sampling. As judged by the metal–carbonyl band intensities, about 80% conversion of the reactant (ν_{CO} = 1977, 1907 cm^{-1}) to monosubstituted product (ν_{CO} = 1907, 1857 cm^{-1}) occurred within 70 min, but after this, a side product with ν = 1892 cm^{-1}, matching the reported frequency of *trans*-$(PPh_3)_2(CO)_4Cr$,[29] increased in prominence, leading to discontinuation of the photolysis. The dark red solution was passed through filter pulp and evaporated. The resulting oil was dissolved in ca. 5 mL of CH_2Cl_2, and the mixture was treated with hexanes to give a solid, which was washed with hexanes and redissolved in a minimum of CH_2Cl_2 before loading onto a hexane-slurry-packed 25 × 2.5 cm silica gel column. Elution with 3:1 hexanes/CH_2Cl_2 removed the starting materials and the side product with the 1892-cm^{-1} absorption. Subsequent elution with pure CH_2Cl_2 gave an orange band which when evaporated gave 0.45 g (57% yield) of red, microcrystalline **5**: mp 184–185 °C; ^1H NMR ($CDCl_3$) δ = 7.87 (1H, d, $J_{HH'}$ = 7.5 Hz, uncomplexed ring), 7.59 (1H, d, $J_{HH'}$ = 7.5 Hz, uncomplexed ring), 7.52–7.40 (8H, m, uncomplexed ring and phosphine arenes), 7.40–7.27 (9H, m, uncomplexed arene and phosphine arenes), 5.30–5.22 (1H, m, complexed arene), 4.82–4.68 (3H , m, complexed arene), 3.61 (3H, s, uncomplexed arene COOMe), 3.58 (3H, s, complexed arene COOMe); IR (cyclohexane) ν_{MCO} = 1918, 1869 cm^{-1}, ν_{COOMe} = 1739 (sh), 1728 cm^{-1}; MS *m/e* 640 (base peak 239), calc M + 1 for $C_{36}H_{29}CrO_6P$ 641.1.

Other Monometallic Phosphine Complexes. (9,10-Dihydrophenanthrene)dicarbonyl(triphenylphosphine)chromium (6): 20-min irradiation; orange powder in 21% yield; mp 161 dec; ^1H NMR ($CDCl_3$) δ = 7.5–7.1 (19H, m, uncomplexed arene and phosphine arenes), 5.30 (1H, d, $J_{HH'}$ = 6.4 Hz, complexed arene), 4.96 (1H, d, $J_{HH'}$ = 6.1 Hz, complexed arene), 4.43–4.30 (2H, m, complexed arene), 3.26–3.10 (1H, m, ethylene bridge), 2.90–2.60 (3H, ethylene bridge); IR (cyclohexane) ν_{CO} = 1904, 1856 cm^{-1}; MS *m/e* 550 (base peak 181), calc M + 1 for $C_{34}H_{27}CrO_2P$ 551.1.

(Fluorene)dicarbonyl(triphenylphosphine)chromium (7): 100-min irradiation; orange powder in 22% yield; mp 219 °C dec; ^1H NMR ($CDCl_3$) δ = 7.5–7.2 (19H, m, uncomplexed arene and phosphine arenes), ca. 5.21 (1H, m, complexed arene), 5.14 (1H, d, $J_{HH'}$ = 6.0 Hz, complexed arene), ca. 4.76 (1H, m, complexed arene), ca. 4.30 (1H, m, complexed arene), 3.88 (2H, s, methylene); IR (THF) ν_{CO} = 1897, 1842 cm^{-1}; MS *m/e* 536 (base peak 166), calc M + 1 for $C_{33}C_{25}CrO_2P$ 537.1.

Dimetallic Bis(dicarbonyl triphenylphosphine) Complexes. (Biphenyl-2,2′-dicarboxylic acid dimethyl ester)bis[dicarbonyl(triphenylphosphine)-chromium] (2). Irradiation analogous to that used in the preparation of **5** (above) with ca. 2.5:1 PPh_3/**11** for 50 min gave a dark red oil after filtration and evaporation, which yielded a solid when redissolved in 5 mL of THF and precipitated with hexanes. The orange powder was copiously washed with the latter and then with acetone to remove traces of **5**. Recrystallization from THF/hexane gave 0.32 g (34%) of **2** as a dark red powder: mp 195 °C dec; ^1H NMR ($CDCl_3$) δ = 7.55–7.35 (14H, m, phosphine arenes), 7.35–7.25 (16H, m, phosphine arenes), 5.52 (2H, d, $J_{HH'}$ = 5.9 Hz, arene), ca. 5.12 (2H, m, arene), ca. 4.83 (2H, m, arene), ca. 4.49 (2H, m, arene), 3.58 (6H, s, COOMe); IR (THF) ν_{MCO} = 1905, 1856 cm^{-1}, ν_{COOMe} = 1735, 1719 cm^{-1}; MS *m/e* 1011 (base peak 185), calc M + 1 for $C_{56}H_{44}Cr_2O_8P_2$ 1011.1.

Other Dimetallic Complexes. (9,10-Dihydrophenanthrene)bis[dicarbonyl(triphenylphosphine)chromium] (3). A 0.40-g sample of **12** and 0.50 g of PPh_3 irradiated for 60 min gave an orange powder (after precipitation of the red oil from THF/hexanes), which was copiously washed first with hexanes and then 3:1 hexanes/acetone. Recrystallization from THF/hexanes gave 0.17 g (21%) of **3** as a red powder: mp >250 °C; ^1H NMR ($CDCl_3$), δ = 7.43–7.37 (12H, m, phosphine arenes), 7.30–7.27 (18H, m, phosphine arenes), 4.97 (2H, d, $J_{HH'}$ = 6.6 Hz, arene), 4.92 (2H, d, $J_{HH'}$ = 6.1 Hz, arene), ca. 4.46 (2H, m, arene), ca. 4.30 (2H, m, arene), 3.20 (2H, d, $J_{HH'}$ = 10.1 Hz, methylene bridge), 2.57 (2H, d, $J_{HH'}$ = 10.2 Hz, methylene bridge); IR (THF) ν_{CO} = 1887, 1840 cm^{-1}.

(Fluorene)bis[dicarbonyl(triphenylphosphine)chromium] (4). Irradiation of 0.30 g of **13** and 0.50 g of PPh_3 for 35 min, washing of the orange powder with hexanes and then acetone, and recrystallization from THF/hexanes gave 0.20 g (12%) of dark red **4**: mp >2.50 °C; ^1H NMR (C_6D_6) δ = 7.59–7.50 (14H, m, phosphine arenes), 7.05–6.94 (16H, m, phosphine arenes), ca. 4.70 (4H, m, arene), 4.44 (2H, m, arene), 4.08 (2H, m, arene), 3.76 (2H, s, methylene); IR (THF) ν_{CO} = 1890, 1843 cm^{-1}.

Results

A. Overall Strategy of Study. The steric constraints introduced by the bis ortho substitution of complex **2** ensures that the phenyl rings will be nearly orthogonal, leading to maximum decoupling of their π systems. The dihedral torsional angle of the $Cr(CO)_3$ analogue of **2** is 100°.[30] The other extreme, that of coplanar bridging ligand π systems, is present in the fluorene complex **4** (assumed torsion of 0°). The ethylenyl annelation of the dihydrophenanthrene complex **3** allows modest deviation from coplanarity. This is measured as ca. 17° in the solid state,[31] and if the data on 9,10-dihydrophenanthrene are taken as a guide,[7a] a similar torsion should exist in solution. Repeated attempts to grow X-ray-quality crystals of the various phosphine derivatives failed, but the tricarbonyl complexes were better behaved. The solid-state structure of (biphenyl-2,2′-dicarboxylic acid dimethyl ester)bis(tricarbonylchromium) (**11**) is from an earlier report.[30] A summary of the X-ray studies of **3** by Dr. John L. Hubbard is available.[9] An ORTEP drawing of **3** is included here as Figure 1.

Introduction of the PPh_3 ligand was intended to stabilize the oxidation products, including the dinuclear dications. The phosphine ligand has the additional advantage of providing a nucleus (^{31}P, $I = {}^1/_2$, 100% abundance) with a hyperfine spin label for ESR experiments. The goal of cation stabilization was achieved, even though some of the experiments had to be conducted at severely reduced temperatures to allow for prolonged spectral monitoring of the oxidation products.

Mononuclear analogues of **2–4** were studied as models for valence-localized Cr(I) monocations. Chart 1 gives structures and numbers for all the compounds included in this study.

B. Electrochemistry. 1. (Arene)Cr(CO)$_3$ Complexes. Data on the oxidation potentials of mono- and dinuclear $Cr(CO)_3$ compounds prepared as part of this study are recorded in Table 1. Compounds **9** and **12** have previously been studied in propylene carbonate.[32]

The oxidation of (arene)$Cr(CO)_3$ complexes has been extensively reported;[33] the 17-electron cations are not generally stable.

(22) Rausch, M. D. *J. Org. Chem.* **1974**, *39*, 1787.
(23) Schloegl, K.; Schoelm, R. *Monatsh. Chem.* **1980**, *111*, 259.
(24) Bitterwolf, T. E.; Herzog, R.; Rockswold, P. D. *J. Organomet. Chem.* **1987**, *320*, 197.
(25) Rieke, R. D.; Tucker, I.; Milligan, S. N.; Wright, D. R.; Willeford, B. R.; Radanovich, L. J.; Eyring, M. W. *Organometallics* **1982**, *1*, 938.
(26) Fischer, E. O.; Kriebitzsch, N. *Z. Naturforsch.* **1960**, *15B*, 465.
(27) Top, S.; Jaouen, G. *J. Organomet. Chem.* **1979**, *182*, 381.
(28) Following the procedure of: Ceccon, A.; Gambaro, A.; Venzo, A.; Lucchini, V. V.; Bitterwolf, T. E.; Shade, J. *J. Organomet. Chem.* **1987**, *327*, 55.
(29) (a) Magee, T. A.; Matthews, C. N.; Wang, T. S.; Wotiz, J. H. *J. Am. Chem. Soc.* **1961**, *83*, 3200. (b) Cotton, F. A.; Kraihanzel, C. S. *J. Am. Chem. Soc.* **1962**, *84*, 4432.
(30) Halwax, G. E.; Voellenkle, H. *Monatsh. Chem.* **1983**, *114*, 687 (or: Schloegl, K.; Schoelm, R. *J. Organomet. Chem.* **1980**, *194*, 69).
(31) Hubbard, J. L.; Pierce, D. T.; Geiger, W. E. Unpublished results at the University of Vermont.
(32) Rieke, R. D.; Milligan, S. N.; Schulte, L. D. *Organometallics* **1987**, *6*, 699. See also ref 25.
(33) For leading references see: Stone, N. J.; Sweigart, D. A.; Bond, A. M. *Organometallics* **1986**, *5*, 2553.

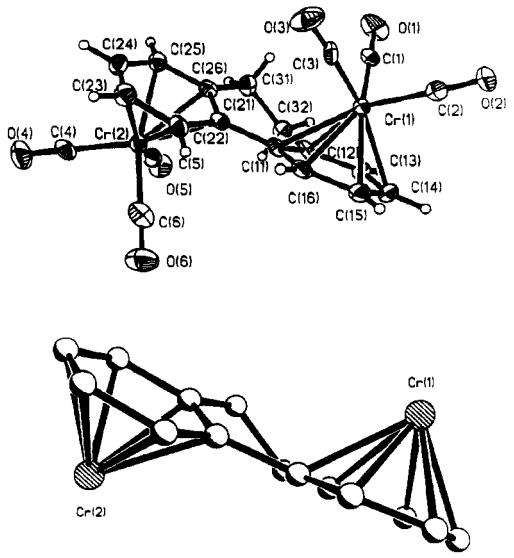

Figure 1. Views of compound **3** from X-ray data of Dr. John Hubbard: (top) ORTEP diagram; (bottom) view emphasizing dihedral twist of biphenyl group (17.9°).

Chart 1

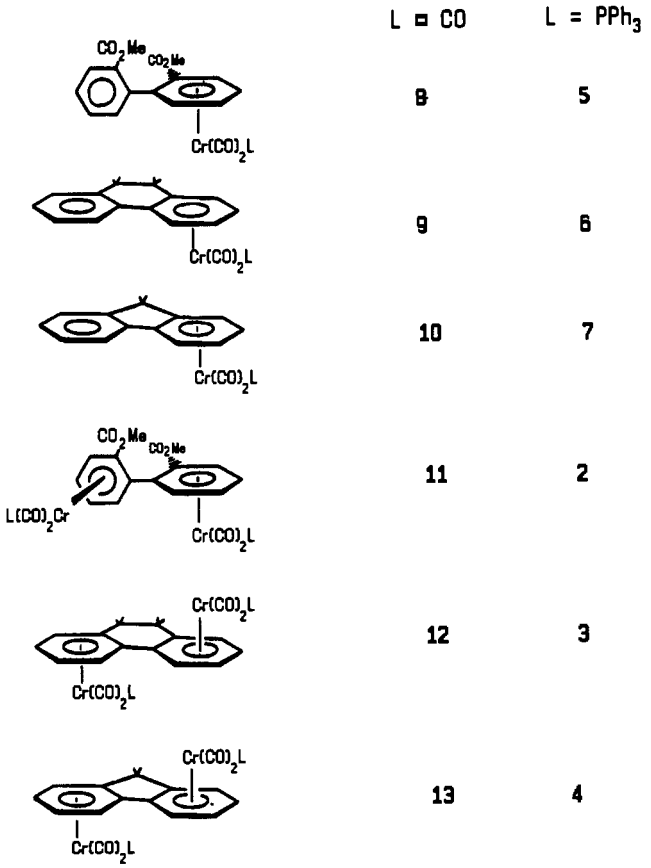

In this study, moderately fast-scan voltammetry was sufficient to outrun the decomposition reactions in most cases and allow measurement of $E°$ potentials of the $Cr(CO)_3$ complexes. For example, complex **11** gave two chemically reversible oxidations at T = 263 K and v = 50 V/s. The two apparent one-electron processes $\mathbf{11}/\mathbf{11}^+$ and $\mathbf{11}^+/\mathbf{11}^{2+}$ were separated in their formal potentials by ca. 130 mV (Table 1). In addition to the general problem of decomposition reactions of the Cr(I) species, dinuclear *di*cations are prone to precipitation in CH_2Cl_2. In the cases of compounds **12** and **13**, this limited the accuracy with which the potential of the second oxidation could be measured. Representative data follow, and further details may be found in ref 9.

Table 1. Electrochemical Data for (Biaryl)$[Cr(CO)_2L]_{1,2}^{0/+/2+}$ Couples (L = CO, PPh_3) in CH_2Cl_2/0.1 M $[Bu_4N][PF_6]$[a]

	0/+ couple			+/2+ couple	
complex	$E°_1$, V	n, equiv mol^{-1}	k_c, s^{-1}	$E°_2$, V	$\Delta E°$, mV
2	–0.12	1.0		+0.13	250
3	–0.28	1.0		–0.01	270
4	–0.21	1.0		+0.06	270
5	–0.03	1.1	1.0(4)		
6	–0.29	1.0			
7	–0.31	1.0			
8	+0.54	[1]	8.3(5)		
9	+0.38	[1]	5.6(5)		
10	+0.35	[1]	2.3(3)		
11[b]	+0.62	[1]	>1.0	+0.75	130
12	+0.42	[1]	>1.0	*c*	*c*
13	+0.41	[1]	>1.0	*c*	*c*

[a] Table columns: formal potentials for 0/+ couple ($E°_1$) and +/2+ couple ($E°_2$) in volts versus Fc; n, apparent n values determined by bulk coulometry at 213 K (square brackets denote n values estimated only from CV characteristics); k_c, first-order decomposition rate constant of cation radical at 298 K (values in parentheses represent ± error limits to the last reported digit); $\Delta E°$, potential separation between formal potentials of 0/+ and +/2+ couples. [b] T = 263 K. [c] Data for bimetallic +/2+ couple was affected by precipitation of dication; see text for description.

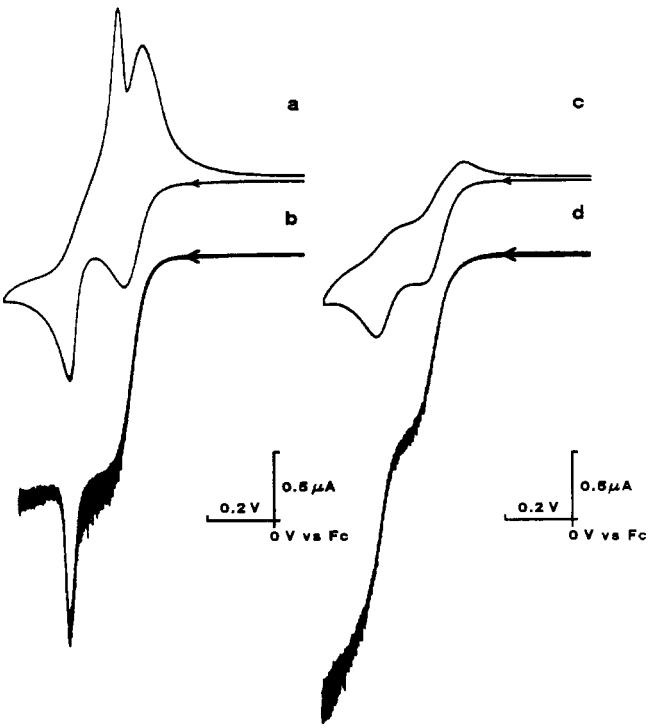

Figure 2. CV scans at Pt (a, c; scan rate 0.05 V/s) and RPE scans (b, d) of 0.40 mM **13** at T = 233 K: left, with CH_2Cl_2; right, after adding 20% v/v propylene carbonate. Scans begin at zero current.

Oxidation of $(fluorene)Cr_2(CO)_6$ (**13**) in CH_2Cl_2 at 233 K proceeds in two one-electron steps. The first oxidation process, involving $\mathbf{13}/\mathbf{13}^+$, is chemically reversible when the scan is clipped before onset of the second wave (i_c/i_a = 0.96, ΔE_p = 74 mV, $E_p - E_{p/2}$ = 60 mV at v = 0.05 V/s). The second wave is apparently also a one-electron process, but the narrow anodic peak (Figure 2, left top) and the sharp reverse peak are consistent with precipitation of the dication $\mathbf{13}^{2+}$ on the electrode and its subsequent cathodic stripping in the return direction of the scan. The hydrodynamic traces recorded at a rotating Pt electrode (RPE) scan (Figure 2, left bottom) are also diagnostic of partial electrode passivation in the vicinity of the second wave. Addition to the solution of the more polar solvent propylene carbonate eliminated precipitation of the dication but enhanced the

Table 2. IR Carbonyl Stretching Frequencies and Integrated Absorption Intensities for (Biaryl)$[Cr(CO)_2PPh_3]_{1,2}^{0/+/2+}$ Complexes[a]

		0 state		+ state[b]			2+ state		
complex	assignment	ν, cm^{-1}	$10^{-3}A_i$, M^{-1} cm^{-2}	ν, cm^{-1}	$10^{-3}A_i$, M^{-1} cm^{-2}	$\Delta\nu$, cm^{-1}	ν, cm^{-1}	$10^{-3}A_i$, M^{-1} cm^{-2}	$\Delta\nu$, cm^{-1}
2	M_1CO, sym	1900	129	1996	41	96	2012	73	112
	M_1CO, asym	1847	94	1913	30	66	1932	50	85
	M_2CO, sym			1910	58	10			
	M_2CO, asym			1863	58	16			
	COOMe	1720	17	1733	10	13	1733	18	13
	COOMe			1712	10	−8			
3	M_1CO, sym	1875	121	1974	68	99	1994	84	119
	M_1CO, asym	1824	98	1875	64	51	1902	80	78
	M_2CO, sym			1894	157	19			
	M_2CO, asym			1850	89	26			
4	M_1CO, sym	1875	129	1972	69	97	1994	87	119
	M_1CO, asym	1822	97	1876	60	54	1894	93	72
	M_2CO, sym			1895	181	20			
	M_2CO, asym			1853	106	31			
5	MCO, sym	1898	49	2001	38	103			
	MCO, asym	1843	47	1971	35	74			
	COOMe	1721	*c*	1740	12	19			
	COOMe	1716	*c*	1715	9	−1			
6	MCO, sym	1879	49	1983	39	104			
	MCO, asym	1821	49	1881	47	60			
7	MCO, sym	1877	55	1985	45	108			
	MCO, asym	1821	45	1883	48	62			

[a] All data obtained from spectra collected at 203 K. Table columns: ν, absorbance peak position; A_i, integrated absorption intensity, $\Delta\nu$, shift of assigned peak from its position in the 0 oxidation state of the complex. [b] Data for bimetallic species were determined from Lorentzian line shape simulations. [c] Peak was not sufficiently resolved for accurate integration.

Table 3. Frozen-Solution (77 K) ESR Data for (Biaryl)$[Cr(CO)_2PPh_3]_{1,2}$ Cation Radicals Generated by Chemical Oxidation in 1:1 v/v $CH_2Cl_2/C_2H_4Cl_2$ or 2:1 v/v THF/CH_2Cl_2[a]

complex	g_1	g_2	g_3	$A_{P,1}$, G	$A_{P,2}$, G	$A_{P,3}$, G
2^+	2.100	2.033	1.992	25	36	29
3^+	2.097	2.030	1.991	27	33	31
4^+	2.100	2.030	1.991	*b*	35	30
5^+	2.100	2.034	1.991	28	33	31
6^+	2.108	2.038	1.994	31	34	32
7^+	2.108	2.035	1.993	27	34	32

[a] Table columns: g_n, g values, and $(A_{P,n})$, ^{31}P nuclear hyperfine coupling constants, for each rhombic **g** tensor ($n = 1$–3). [b] Hyperfine coupling was poorly resolved; see text for description.

decomposition reactions of both the mono- and the dication (Figure 2, right). Complex **12** gave similar results. The potentials of oxidation of all $Cr(CO)_3$ compounds are collected in Table 1, along with estimates, where possible, of the rate constant for decomposition of the Cr(I) system.

2. Mononuclear (Arene)$Cr(CO)_2(PPh_3)$ Complexes. As noted in a number of earlier studies,[34] the 17e⁻ cations of the dicarbonyl phosphine complexes displayed greatly enhanced stabilities over those of the corresponding tricarbonyl complexes. Results of cyclic and RPE voltammetries as well as controlled-potential coulometry establish one-electron oxidations for compounds **5**–**7** (Table 1) to monocations sufficiently stable to characterize by IR and ESR spectroscopies (Tables 2 and 3). The least stable monocation of this type was 5^+, in which the arene is 2,2′-(dimethyl ester)biphenyl. This complex required CV scan rates above 10 V/s at 298 K for complete chemical reversibility, and the lifetime of 5^+ was calculated[35] as ca. 0.5 s using data both from CV scans and double potential step chronoamperometry.[9] Complete chemical reversibility was attained at low scan rates below 263 K. Bulk coulometry at 213 K gave 1.07 faradays/mol and a red solution showing the presence of the 17e⁻ system 5^+ in ESR and IR spectra. The $E°$ of $5/5^+$ (−0.03 V) is positive of those of (biphenyl)$Cr(CO)_2(PPh)_3$ (−0.14 V)[6] and of both **6** and **7**, reflecting the effect of the electron-withdrawing CO_2Me substituent on the arene ring. The monocations of **6** and **7** were quite persistent and presented no problems for in situ characterization.

3. Dinuclear (Arene)$[Cr(CO)_2(PPh_3)]_2$ Complexes. With a second metal center coordinated to the diaryl backbone, complexes **2**–**4** demonstrated one additional oxidation wave about a quarter of a volt more positive than the first. The lifetimes of the *mono*cations of **2**–**4** were about the same as those of the corresponding mononuclear compounds **5**–**7**; i.e., no additional chemical stability was imparted to monocations of dinuclear systems. Since the cations of the dinuclear systems are the key species in this study, we now offer more detailed information on their properties and characterization.

The two essentially Nernstian[36] one-electron oxidations were chemically reversible for complexes **3** and **4** at ambient temperatures and for **5** at low temperatures. The CV scan in Figure 3 (complex **4**, $T = 213$ K) is representative. The $\Delta E°$ values of the couples ($\Delta E° = E°_2 - E°_1$) were 250–270 mV (Table 4). For all three compounds, controlled-potential bulk coulometry below 220 K at an applied voltage, E_{appl}, of $(E°_2 + E°_1)/2$ produced red solutions of the monocations in over 90% yield (judging by RPE plateau currents) with the expected 1.0 ± 0.1 faradays passed per mole of complex. ESR spectra of these solutions (frozen at 77 K) matched those produced by chemical oxidation of the same compounds (vide infra). When the red solutions were electrochemically bulk-reduced, the original complexes were regenerated in at least 75% overall yield. The generation of 2^+ was compromised by spontaneous regeneration of the neutral complex, so that after passage of 1.0 faraday/mol, the solution contained ca. 25% 2^+ and 75% **2**.

Decomposition through regeneration of the lower oxidation state also affected attempts to generate *di*cations of the dinuclear complexes. In some cases, the dications decomposed in part to the corresponding monometallic complexes; e.g., 2^{2+} gave some

(34) (a) Connelly, N. G.; Demidowicz, Z. *J. Organomet. Chem.* **1974**, *73*, C31. (b) Connelly, N. G.; Demidowicz, Z.; Kelly, R. L. *J. Chem. Soc., Dalton Trans.* **1975**, 2335.

(35) A first-order decomposition reaction was assumed, and the ratio of i_c/i_a vs scan rate was used to calculate the apparent half-life of the cation, using the method in: Nicholson, R. S. *Anal. Chem.* **1966**, *38*, 1406.

(36) The peak potential separations were within 10 mV of those measured for the ferrocene/ferrocenium couple under identical conditions. Typically these were 70–90 mV for low temperatures and scan rates.

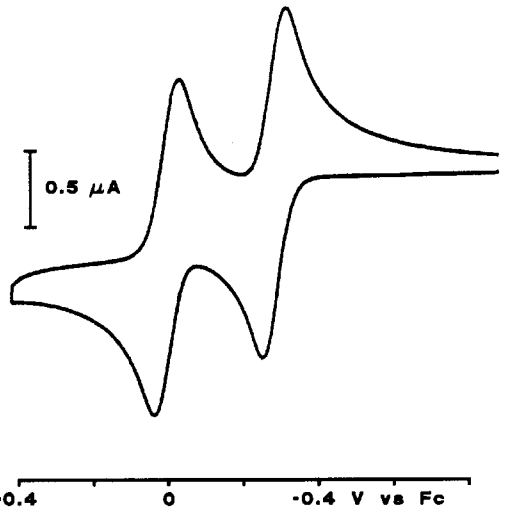

Figure 3. CV scan (v = 0.20 V/s) of 0.49 mM **4** in CH_2Cl_2/0.1 M $[Bu_4N][PF_6]$ at 213 K.

Table 4. Summary of Electrochemical, Infrared, and ESR Data for (Biaryl)$[Cr(CO)_2PPh_3]_{1,2}$ Complexes[a]

complex	$\Delta E°$, mV	$\Delta\nu_{sym}$, cm^{-1}	$\Delta\nu_{asym}$, cm^{-1}	$\langle A_P\rangle$,[b] G	$\angle_{torsion}$, deg	d_{M-M}, Å
2	250	96	16	30	111	4.69
3	270	99	26	30	18	5.45
4	270	97	31	*c*	0	5.63
5		103	74	31		
6		104	60	32		
7		108	62	31		

[a] Table columns, $\Delta E°$, voltage separation between formal potentials of 0/+ and +/2+ couples; $\Delta\nu_{sym}$, shift of highest energy symmetric MCO stretching peak, and $\Delta\nu_{asym}$, shift of lowest energy asymmetric MCO stretching peak, for 0/+ oxidation; $\langle A_P\rangle$, calculated average of ^{31}P nuclear hyperfine coupling constants ($A_{P,n}$) for rhombic **g** tensors (n = 1–3) of cation radicals; $\angle_{torsion}$, biaryl torsion angle; d_{M-M}, intermetallic distance calculated from structural determination of (biaryl)$[Cr(CO)_3]_2$ complexes. [b] Corresponding cations. [c] See text.

5. In light of these difficulties, we employed a low-temperature flow-cell with chemical oxidants to obtain IR spectra of the dications.

C. IR Spectra. Vibrational spectra may provide direct evidence for or against intrinsic electronic delocalization of a mixed-valent ion. High-quality IR spectra were obtained for each of the mono- and dications of the phosphine-substituted complexes. Solutions of the dinuclear dications were kept below 200 K during spectral acquisition. We report the oscillator strengths of Cr–CO bands in Table 2 and show molar absorptivities in the figures. Simulation procedures were employed to assign contributions from overlapping spectral bands.

1. Mononuclear (Arene)$Cr(CO)_2(PPh_3)$ Cations. Figure 4 reproduces IR spectra of **5** and **5**$^+$. The latter is the least stable cationic member of this series. Yet, efficient production of it is achieved at 203 K when the neutral complex is oxidized by 1 equiv of $Ni(tfd)_2$. The spectrum of **5** (top) has two M–CO bands at ν_{sym} = 1898 cm^{-1}, ν_{asym} = 1843 cm^{-1} and a single ester carbonyl band at ν_{COOMe} = 1716 cm^{-1}. The monocation **5**$^+$ has *two* ester CO bands, at 1740 and 1715 cm^{-1}, the former being assigned to the CO_2Me group on the metal-complexed arene, on the basis that the shift of +25 cm^{-1} originates from the poorer electron-withdrawing character of the Cr(I) atom, compared to the original Cr(0). The pattern of two M–CO bands shifted to higher energy by ca. 100 cm^{-1} (ν_{sym} = 2001 cm^{-1}, ν_{asym} = 1917 cm^{-1}) is as observed for other Cr(0) → Cr(I) oxidations.[6,34,37] The band assigned to the asymmetric stretch is considerably broader than its symmetric counterpart, but the integrated intensities are approximately the same. After about 5 min in the IR cell, the spectra showed evidence of decomposition.[38]

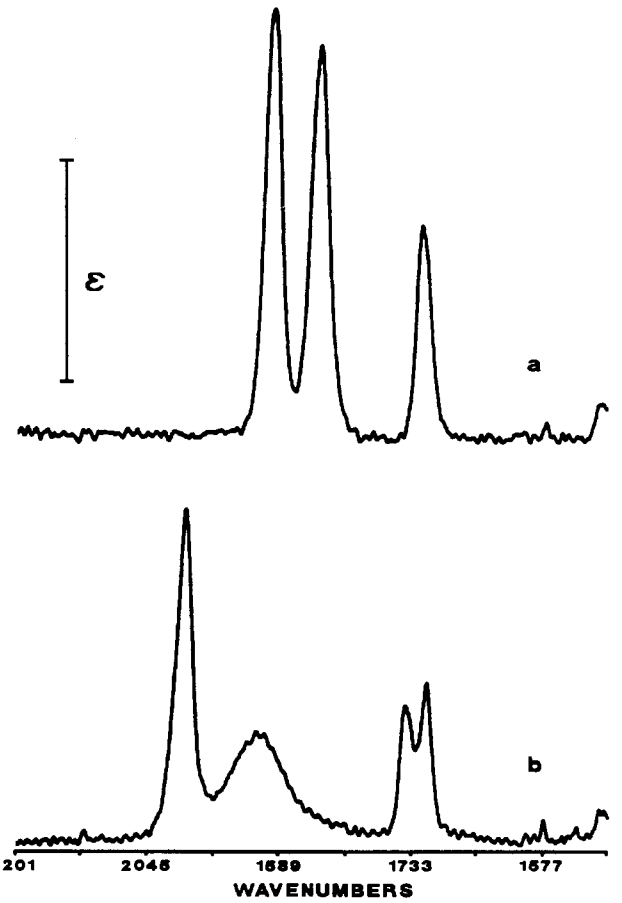

Figure 4. IR spectra of 2.27 mM (a) **5** and (b) **5**$^+$ in CH_2Cl_2 at 203 K. $\epsilon = 10^{-3}$ M^{-1} cm^{-1}.

The monocation **5**$^+$ was reduced back to **5** by addition of a slight molar excess of decamethylferrocene, Cp^*_2Fe, to the reaction solution. Since the $E°$ of $Cp^*_2Fe^{+/0}$ is negative of all those of the Cr compounds in this study, the Fe(II) complex, which is IR-silent in the CO spectral range, is a convenient reductant for the oxidized Cr compounds. The spectrum of **5** in Figure 4 was obtained by means of this back-reduction method. Results for the other mononuclear complexes are listed in Table 2.

2. Dinuclear (Arene)$[Cr(CO)_2(PPh_3)]_2$ Mono- and Dications. Complex 2. One molar equivalent of $Ni(tfd)_2$ quantitatively oxidized a CH_2Cl_2 solution of **2** to its monocation (Figure 5b). Trapped valency in **2**$^+$ is immediately evident from the splitting of the ester CO band into a pair at 1733 and 1712 cm^{-1}, the former assigned to the substituent on the Cr(I)-complexed arene and the latter to that on the Cr(0) arene. Oxidation to the dication **2**$^{2+}$ by a second equivalent of oxidant gave a darker red solution in which the ester CO frequencies are again equivalent (Figure 5c) and characteristic of two Cr(I)-complexed arenes (ν_{COOMe} = 1733 cm^{-1}).

The conclusion of trapped valence in **2**$^+$ is supported by consideration of the metal carbonyl frequencies. Both the neutral and twice-oxidized compounds, **2** and **2**$^{2+}$, show *pairs* of M–CO bands, shifted to appropriately higher energies (Figure 5a,c). However, the one-electron intermediate, **2**$^+$, has *three* major features arising from superposition of the *band pairs* of the Cr(I)

(37) Merkert, J. W.; Geiger, W. E.; Paddon-Row, M. N.; Oliver, A. M.; Rheingold, A. L. *Organometallics* **1992**, *11*, 4109.

(38) It is important to note that the solutions of the cations in the reaction vessel showed no evidence of decomposition over this time period, providing a stable reservoir for back-reduction of the cations to the neutral compounds.

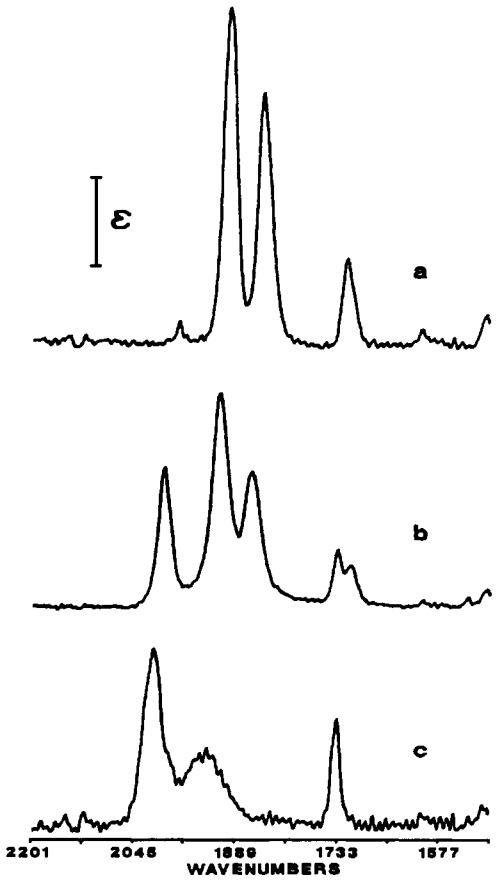

Figure 5. IR spectra of (a) 1.19 mM **2**, (b) 2.27 mM $\mathbf{13}^{+}$, and (c) 1.19 mM $\mathbf{13}^{2+}$ in CH_2Cl_2 at 203 K.

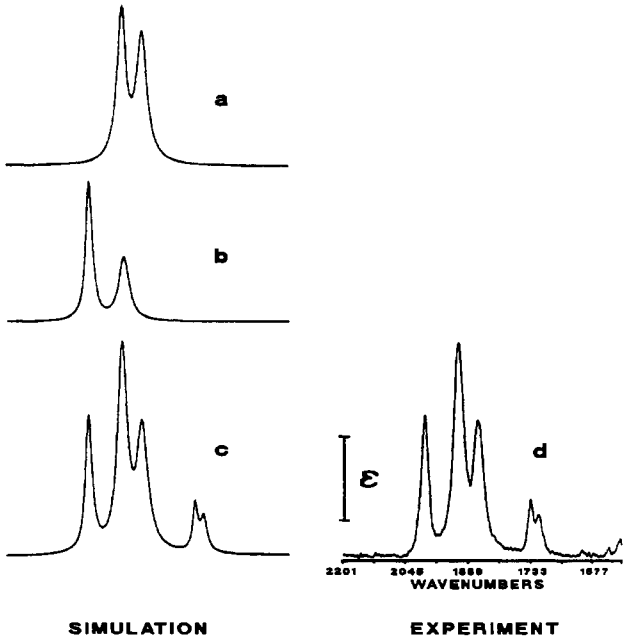

Figure 6. Computed line-shape fit (c) for the experimental IR spectrum (d) of 2.27 mM $\mathbf{13}^{+}$ in CH_2Cl_2 at 203 K. Contributions in (a) and (c) represent the features assigned to the Cr(0) and Cr(I) sites, respectively.

and Cr(0) sites. The 1800–2000-cm^{-1} region was adequately fit by line-shape analysis (Figure 6) assuming overlap of the ν_{sym} Cr(0) and ν_{asym} Cr(I) features, which has ample precedent.[6,37,39] The frequencies and intensities yielding the apparent best fit between observed and simulated spectra are listed in Table 2.

(39) Geiger, W. E.; Van Order, N., Jr.; Pierce, D. T.; Bitterwolf, T. E.; Rheingold, A. L.; Chasteen, N. D. *Organometallics* **1991**, *10*, 2403.

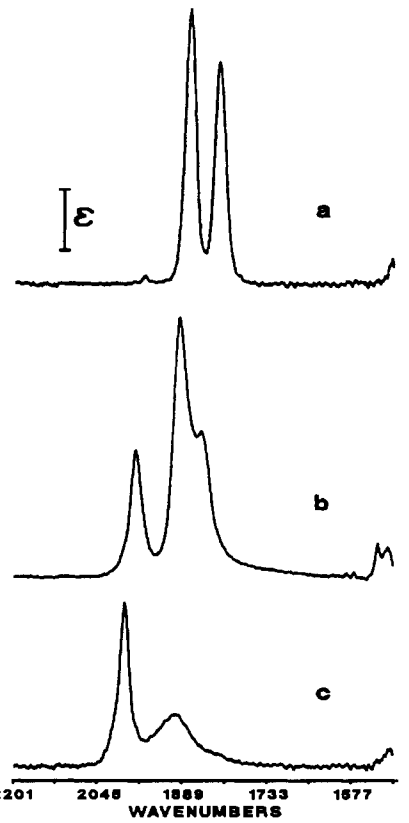

Figure 7. IR spectra of (a) 1.12 mM **3**, (b) 2.27 mM $\mathbf{3}^{+}$, and (c) 1.12 mM $\mathbf{13}^{2+}$ in CH_2Cl_2 at 203 K.

The values of the two overlapping components are, of course, the least precise.

Complexes 3 and 4. Results for these complexes were also consistent with the description $Cr^0Cr^0 \rightarrow Cr^ICr^0 \rightarrow Cr^ICr^I$ in the electron-transfer series. The outlying oxidation states showed the expected two M–CO bands (Figures 7 and 8). Spectra of the monocations, however, were more poorly resolved than that of $\mathbf{2}^{+}$, owing to the fact that, by comparison, the Cr(I)–CO pair is shifted *less than* that of **2** and the Cr(0)–CO pair is shifted *more than* that of **2**. In the context of **3** (Figure 7, middle), the bands at 1974 and 1850 cm^{-1} are readily assigned to Cr(I) ν_{sym} and Cr(0) ν_{asym}, respectively; the intermediate-energy features required simulation procedures (Figure 9) and gave 1894 and 1875 cm^{-1} for the other two features. For the fluorene complex, the spectrum of the mixed-valent ion $\mathbf{4}^{+}$ barely shows a third feature as a shoulder (Figure 8, middle), so that the middle two CO frequencies are not precisely known. Table 2 gives the apparent best fit.

Our interpretation of the significance of the energy shifts of the CO bands is delayed until after brief description of the ESR results. Clearly, though, the IR spectra of $\mathbf{2}^{+}$, $\mathbf{3}^{+}$, and $\mathbf{4}^{+}$ support a *trapped-valent* Cr^ICr^0 formulation for the dinuclear monocations. Furthermore, the trapped valency does not appear to arise from ion-pairing effects, since oxidation with either [Fc][PF_6] or $Ni(tfd)_2$ give identical spectra for $\mathbf{4}^{+}$. We do *not* expect that the two counterions from these preparations, namely PF_6^- and, especially, $Ni(tfd)_2^-$, strongly ion-pair with $\mathbf{4}^{+}$.

D. ESR Spectra. Electron spin resonance spectra were readily obtained on frozen solutions (77 K) of monocations of both mono- and dinuclear species, prepared either by chemical oxidation [Cp_2Fe^+ or $(p\text{-}BrC_6H_4)_3N^+$] or by anodic electrolysis. The results were in all cases diagnostic of a single Cr(I) site, with rhombic g tensors and ^{31}P hyperfine splittings (hfs) like those of other 17e$^-$ (arene)$Cr(CO)_2(PR_3)^+$ systems.[6,34,37] (Table 3). Figure 10 shows a typical spectrum (for $\mathbf{3}^{+}$), from which three sets of doublets arising from interaction with a single P atom are evident, as

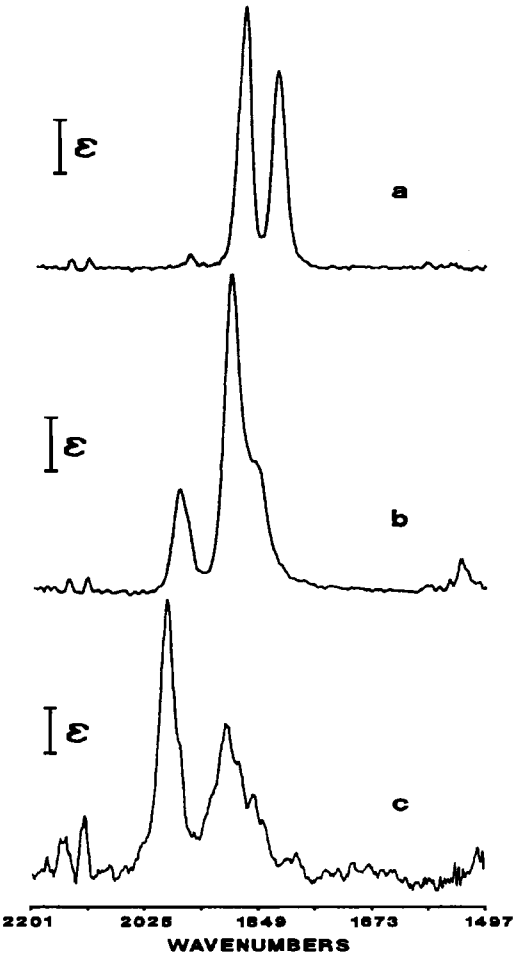

Figure 8. IR spectra of (a) 0.926 mM **4**, (b) 0.926 mM 4^+, and (c) 0.125 mM 4^{2+} in CH_2Cl_2 at 203 K.

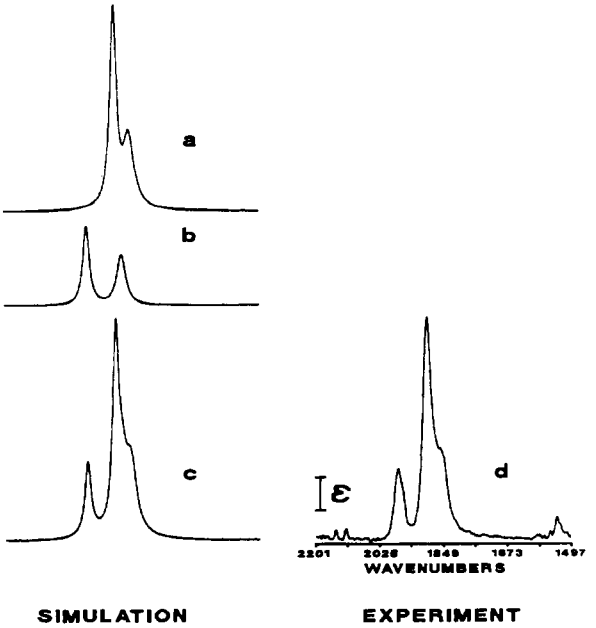

Figure 9. Computed line-shape fit (c) for 4^+, with the Cr(0) and Cr(I) components, (a) and (b), respectively, shown, analogous to Figure 6.

expected for a trapped-valent complex. The increasing line breadth from low to high field is typical of this family of radicals.[34,37]

The only unusual feature among all the spectra was that found in the low-field region of 4^+, which was suggestive of more than two lines in the g_1 region of this radical (Figure 11). This

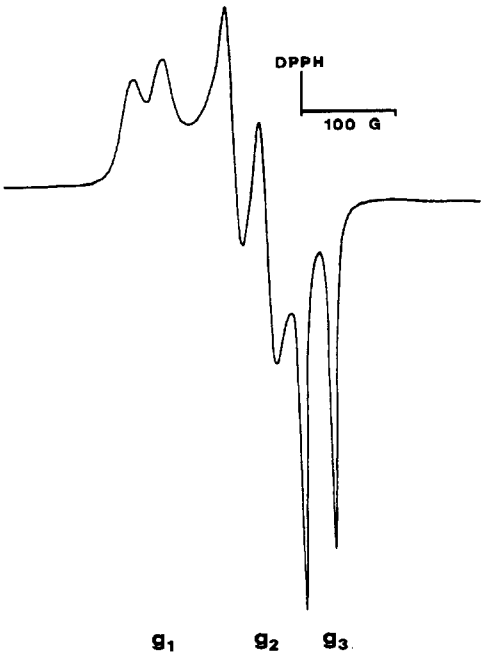

Figure 10. ESR spectrum of 6^+ in 2:1 THF/CH_2Cl_2 at 77 K, generated by oxidation of a 1.96 mM solution of **6** with Fc^+.

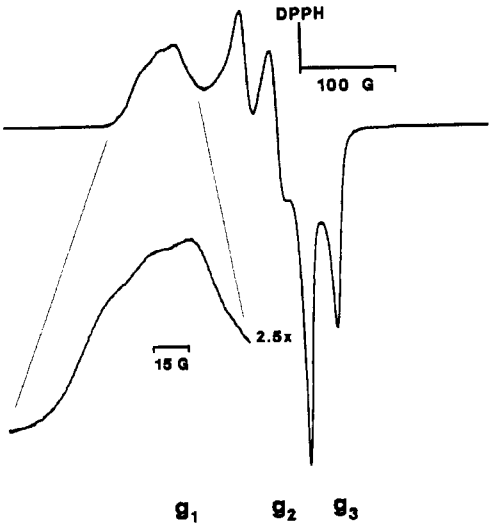

Figure 11. ESR spectrum of 4^+ in 2:1 THF/CH_2Cl_2 at 77 K, generated by oxidation of a 0.99 mM solution of **4** with Fc^+.

characteristic was reproduced under many different conditions of radical preparation and was unaltered by successive thawing and refreezing of the sample, making a secondary radical an improbable reason for the shape of the peak. If an interaction with a *second* P atom is involved in 4^+, the splitting would have to be quite anisotropic, since no unusual features are seen in the more highly resolved g_2 and g_3 regions. We therefore do not favor this interpretation. The origin of the distortion of the low-field feature of 4^+ remains unclear.

Owing to fast relaxation effects[6,46] none of these radicals exhibited fluid solution spectra with the exception of 4^+, which gave a single broad line, $g_{iso} \approx 2.03$, varying in half-width from 65 to 125 G over the temperature range 203–243 K. At higher temperatures, the signal was not detected.

Discussion

A. Categorization of Mixed-Valent Ions. Although IR and ESR spectra of 2^+–4^+ establish the trapped valency of the formal Cr^ICr^0 ions, both the modest $\Delta E°$ values of the dinuclear systems (ca. 260 mV) and the change of ν_{MCO} in *both* the 0/1+ and

1+/2+ couples argue that the two metals are not electronically insulated from each other. A description of the ions as moderately-interacting class II systems[40] seems appropriate.

B. Trapped Valency Independence of Degree of Biphenyl Twist. The present data show that even when the bridging biphenyl has maximum overlap of its π systems, the half-filled orbital in the formal mixed-valent ion is *not* distributed over both metals. That is, these formal d^5–d^6 systems *do not* exhibit intrinsic delocalization. This is in contrast to complex $\mathbf{1}^+$ and its (diphenylarsino)-methane-bridged analogue, which appear to possess intrinsic delocalization. The valence trapping that is seen for $\mathbf{4}^+$, which has coplanar phenyl bridges, implies that the electronic delocalization mechanism in $\mathbf{1}^+$ is unlikely to involve the bridging π system. Since fast electron transfer though the dppm bridge is also unlikely, the delocalization in $\mathbf{1}^+$ is likely to involve direct interaction of the two metals, through space, even though they are separated by well over 4 Å. The lack of significant involvement of the bridging π ligand in the SOMO of the MV ions implies that the orbital makeup of the Cr(I) site may be similar to that of (arene)$Cr(CO)_3$, in which the HOMO is nonbonding between the arene and the metal.[41]

C. Charge Transmission in Mixed-Valent Ions. The valence-trapped description of the mixed-valent ions does not, of course, require the *charge* on the d^5 and d^6 sites to be the same as in the mononuclear d^5 [Cr(I)] or d^6 [Cr(0)] analogues. The molecular framework connecting the two metals is expected to transmit some charge between sites, even if only through the σ framework. Since metal–carbonyl IR frequencies follow changes in metal charge,[42] it is instructive to quantitatively examine the spectral shifts concomitant with successive oxidation steps of **2**–**4**. The highest and lowest energy M–CO bands are used to track this effect, since it is their energies which are precisely known in our results.

The highest energy band, assigned to Cr(0) ν_{sym} in the neutral complexes and Cr(I) ν_{sym} in the two oxidized forms, shifts by +96–99 cm^{-1} in going from the $m = 0$ to $m = 1+$ species (where m is the charge on the molecule) and only an additional 16–22 cm^{-1} in the $m = 1+$ to $m = 2+$ change (Table 4). The partitioning of the IR shifts between the $m = 1+$ and 2+ states shows clearly that the two metal sites are *not* charge-insulated from each other in the dinuclear complexes.

Compounds **2**–**4** show the same shifts in ν_{sym} in proceeding through the sequence of two oxidations. On the other hand, the shift of the *lowest* energy CO band, assigned to Cr(0) ν_{asym} in $m = 0$ and $m = 1+$ species, and to Cr(I) ν_{asym} in $m = 2+$ species, depends clearly on structure. From **2** to **3** to **4**, the ν_{asym} shift in the $m = 0$ to $m = 1+$ step increases from 16 to 26 to 31 cm^{-1}. In fact, when the $m = 0$ to 1+ energy shift of ν_{asym} is considered as a fraction of the *total* shift in the band (from $m = 0$ to $m = 2+$), the increase is even more pronounced. Taking the ratio of $\Delta\nu_{0/1+}/\Delta\nu_{0/2+}$, we obtain 0.19 for **2** (16 cm^{-1}/85 cm^{-1}), 0.33 for **3**, and 0.43 for **4**. In the last of these, the energy increase in ν_{asym} is almost *equally* partitioned between the first and second oxidations.

We interpret the trends in ν_{asym} shifts to be evidence of increased *charge* (not spin) transmission from the Cr(I) site to the Cr(0) site as the dihedral angle of the biphenyl system decreases in this series of mixed-valent ions. Since the bridging π systems are essentially orthogonal in **2** and coplanar in **4**, one may view the small shift in **2** as arising from σ-framework transmission and the additional shifts in **3** and **4** as arising from π-framework transmission.

D. Final Considerations. LeVanda et al. compared two biferrocene derivatives in which the ortho methyl groups provide the steric interference to twist the bridging fulvalene group.[43] In going from R = H to R = Me, a small decrease in $\Delta E°$ was noted (315 to 260 mV). The mixed-valent monocations displayed an intervalence-transfer band of the same energy (5.5×10^3 cm^{-1}), but the band intensity was only about half as large for the twisted monocation. This was ascribed to less effective interactions through the ligand π/π^* orbitals. It would appear that both diiron monocations are trapped-valent species, with the SOMO localized on one redox site (essentially Fe), analogous to our conclusions about the *spin distribution* in the present Cr^ICr^0 biphenyl compounds.

The *charge* distribution in the monocations is not as simple to probe, however. The Fe–Cp ring frequency is reported to be oxidation-state sensitive in going from $CpFe^{II}$ to $CpFe^{III}$,[44] but the changes are rather small and the bands fall in a spectral region that is not amenable to study in many matrix conditions. In contrast, M–CO frequencies may be convenient probes to intramolecular charge effects over relatively long distances. A number of recent papers reported shifts in M–CO frequencies upon oxidation or reduction of a second site separated by several bonds from the metal–carbonyl site.[45]

The present level of quantitative understanding of the CO frequency shifts is fairly primitive, however. The frequency shifts are generally not the same for different fundamental vibrations, at least in these $M(CO)_2$ systems. In the present case, ν_{asym} is far more sensitive to geometry changes (and, perhaps, charge transmission) than is ν_{sym}. The use of ligand spectral shifts to follow charge localization in redox processes would be aided by further experimental work and greater theoretical understanding of this phenomenon.

Acknowledgment. We thank Dr. John Hubbard for permission to quote unpublished results from his X-ray analysis studies of **3** and acknowledge the generous support of the National Science Foundation under Grants CHE86-03728 and 91-16332 to W.E.G. and RII86-10679 to the State of Vermont for purchase of an X-ray diffractometer.

Supplementary Material Available: A description of the construction and operation of a low-temperature, flow-through IR cell, including a diagram (4 pages). Ordering information is given on any current masthead page.

(40) Robin, M. B.; Day, P. *Adv. Inorg. Chem. Radiochem.* **1967**, *10*, 247.
(41) (a) Byers, B. P.; Hall, M. B. *Organometallics* **1987**, *6*, 2319. (b) Guest, M. F.; Hillier, I. H.; Higginson, B. R.; Lloyd, D. R. *Mol. Phys.* **1975**, *29*, 113.
(42) (a) Elschenbroich, Ch.; Salzer, A. *Organometallics: A Concise Introduction*, 2nd ed.; VCH Publishers: Weinheim, Germany, 1992; p 229. (b) Collman, J. P.; Hegedus, L. S.; Norton, J.; Finke, R. G. *Principles and Applications of Organotransition Metal Chemistry*; University Science Books: Mill Valley, CA, 1987; p 114.
(43) Le Vanda, C.; Bechgaard, K.; Cowan, D. O.; Rausch, M. D. *J. Am. Chem. Soc.* **1977**, *99*, 2964.
(44) Dong, T.-Y.; Hendrickson, D. N.; Pierpont, C. G.; Moore, M. F. *J. Am. Chem. Soc.* **1986**, *108*, 963 and references therein.
(45) See leading references in: Miller, T. M.; Ahmed, K. J.; Wrighton, M. S. *Inorg. Chem.* **1989**, *28*, 2347.
(46) A closely-related series of isoelectronic radicals, namely $(C_5R_5)Cr(CO)_2L$ and $CpMn(CO)_2L^+$, L = CO or phosphine, are known to possess nearly-degenerate ground states, leading to rapid electronic relaxation rates and undetectably broad resonances in fluid media. For leading references see: (a) Hoobler, R. J.; Hutton, M. A.; Dillard, M. M.; Castellani, M. P.; Rheingold, A. L.; Rieger, A. L.; Rieger, P. H.; Richards, T. C.; Geiger, W. E. *Organometallics* **1993**, *12*, 117. (b) Fortier, S.; Baird, M. C.; Preston, K. F.; Morton, J. R.; Ziegler, T.; Jaeger, T. J.; Watkins, W. C.; MacNeil, J. H.; Watson, K. A.; Hensel, K.; LePage, Y.; Charland, J.-P.; Williams, A. J. *J. Am. Chem. Soc.* **1991**, *113*, 542. (c) Pike, R. D.; Rieger, A. L.; Rieger, P. H. *J. Chem. Soc., Faraday Trans. 1* **1989**, *85*, 3913.